

# It is feasible to directly measure black hole masses in the first galaxies

Hamsa Padmanabhan<sup>a</sup> and Abraham Loeb<sup>b</sup>

<sup>a</sup>Canadian Institute for Theoretical Astrophysics,  
60 St. George Street, Toronto, ON M5S 3H8, Canada

<sup>b</sup>Astronomy department, Harvard University,  
60 Garden Street, Cambridge, MA 02138, U.S.A.

E-mail: [hamsa@cita.utoronto.ca](mailto:hamsa@cita.utoronto.ca), [aloeb@cfa.harvard.edu](mailto:aloeb@cfa.harvard.edu)

Received January 27, 2020

Accepted February 24, 2020

Published March 13, 2020

**Abstract.** In the local universe, black hole masses have been inferred from the observed increase in the velocities of stars at the centres of their host galaxies. So far, masses of super-massive black holes in the early universe have only been inferred indirectly, using relationships calibrated to their locally observed counterparts. Here, we use the latest observational constraints on the evolution of stellar masses in galaxies to predict, for the first time, that the region of influence of a central supermassive black hole at the epochs where the first galaxies were formed is *directly resolvable* by current and upcoming telescopes. We show that the existence of the black hole can be inferred from observations of the gas or stellar disc out to  $> 0.5$  kpc from the host halo at redshifts  $z \gtrsim 6$ . Such measurements will usher in a new era of discoveries unraveling the formation of the first supermassive black holes based on subarcsecond-scale spectroscopy with the *JWST*, *ALMA*, and the *SKA*. The measured mass distribution of black holes will allow forecasting of the future detection of gravitational waves from the earliest black hole mergers.

**Keywords:** high redshift galaxies, massive black holes, rotation curves of galaxies

**ArXiv ePrint:** [1912.05555](https://arxiv.org/abs/1912.05555)

---

## Contents

<b>1</b>	<b>Introduction</b>	<b>1</b>
<b>2</b>	<b>Quantifying this effect</b>	<b>2</b>
<b>3</b>	<b>Results</b>	<b>2</b>
<b>4</b>	<b>Conclusions</b>	<b>6</b>

---

## 1 Introduction

Massive black holes (with masses of about a million solar masses) are known to exist at the centres of galaxies in the nearby universe. Locally, the masses of such black holes have been measured from their gravitational radius of influence on the motion of stars and gas in their host galaxies. This method was particularly effective for the Milky Way [1–4] and NGC 4258 [5]. Local measurements imply a ratio of the central black hole mass to stellar mass  $M_*$  of the host spheroid to be about  $10^{-4}$ – $10^{-3}$  in the local universe [6, 7].

Supermassive black holes with masses  $M_{\text{BH}}$  of more than a billion solar masses are inferred to exist out to a redshift  $z = 7.54$ , less than  $\sim 700$  million years after the Big Bang [8]. How the seeds for these black holes grew so early in the universe is still an open question [9]. However, there is evidence indicating that at redshifts  $z > 6$ , the central black hole to stellar mass ratio had been more than order of magnitude or two higher [10, 11] than the locally observed value. Theoretical arguments supporting this evolution stem from the inferred black hole-bulge mass relation [12, 13] extrapolated to high redshifts, suggesting that  $M_{\text{BH}}$  grows as a steep function of the halo circular velocity  $v_c$ :  $M_{\text{BH}} \propto v_c^\gamma$  with  $\gamma \sim 5$ .

The evolution of the stellar mass  $M_*$  in dark matter haloes of both early and present-day galaxies is fairly well-constrained. The latest observations from a wide range of surveys, including the Sloan Digital Sky Survey (SDSS), the PRISM Multi-object Survey (PRIMUS), UltraVISTA, the Cosmic Assembly Near-infrared Deep Extragalactic Legacy Survey (CANDELS), and the FourStar Galaxy Evolution Survey (ZFOURGE) all support [14] a well-defined  $M_*(z)$  across the full redshift range,  $0 < z < 10.5$ . The data indicate that the average stellar mass in Milky-Way sized dark matter haloes evolves only by a factor of  $\sim 1.6$  over redshifts  $z \sim 6$  to the present (see figure 9 of ref. [14]).

The above two results, taken together, imply a fascinating conclusion. Since the stellar mass evolves much more modestly than the black hole mass [a trend also found in recent AGN observations from the *Chandra*-COSMOS Legacy Survey; ref. 15], the central black hole mass makes up a much larger fraction of the stellar mass at high redshifts (a fraction of  $\sim 0.3$  at redshift  $z \sim 6$  compared to  $10^{-4}$  at  $z \sim 0$ ). This fact, whose validity has been hinted at in the past [11, 16], is well-supported by the recent *ALMA*<sup>1</sup> spectroscopic study [10] of [CII]-detected quasars at  $z > 6$  which indicates significantly more than two orders of magnitude evolution of the locally observed black hole-bulge mass relation [7].<sup>2</sup> An immediate implication of this finding is that the central black hole should have a measurable

---

<sup>1</sup><https://almascience.nrao.edu/about-alma/alma-basics>.

<sup>2</sup>We also note that the recently discovered class of Obese Black Hole Galaxies [OBGs; 17] can have black hole-stellar mass ratios reaching as high as  $M_{\text{BH}}/M_* \sim 1$  at high redshifts.

influence on the circular velocity profiles of galaxies at high redshift. A couple of caveats to this conclusion, however, are worth noting: it has been pointed out in the literature that the evolution in the black hole-bulge mass relation may be a selection effect [e.g., 18–21], whereas some simulation papers do not find much evolution [e.g., 22–24]. In the following section, we quantify the magnitude of this effect and its observational consequences for current and future generation experiments.

## 2 Quantifying this effect

To quantify this effect, we predict the rotation curves of typical Milky-Way sized haloes at  $z \sim 6$ , separating the dark matter, stellar disc, and black hole components. For the dark matter, we assume a Navarro-Frenk-White [25] profile with the mass  $M_{\text{halo}}(r)$  within radius  $r$  given by [28]:

$$M_{\text{halo}}(r) = 4\pi\rho_{\text{crit}}\delta_0 r_s^3 \left[ \ln(1 + cx) - \frac{cx}{1 + cx} \right] \quad (2.1)$$

where  $\rho_{\text{crit}}$  is the critical density, and  $c = r_{200}/r_s$  is the concentration parameter of the halo, expressed in terms of the limiting radius  $r_{200}$  of the virialized halo and its scale radius  $r_s$ . The term  $x$  denotes the radial distance expressed in terms of the limiting radius:  $x = r/r_{200}$ . The  $\delta_0$  is the characteristic overdensity defined as:

$$\delta_0 = \frac{200}{3} \frac{c^3}{\ln(1 + c) - c/(1 + c)} \quad (2.2)$$

The halo concentration is assumed to be  $c = 3.5$  at  $z = 6$ , consistent with the findings of the recent physically motivated models [26]. For the stellar component, we use an exponential disc profile, with the disc masses within a distance  $r$  from the centre of the galaxy,  $M_d(r)$  given by [28]:

$$M_d(r) = M_d \left[ 1 - \left( 1 + \frac{r}{R_d} \right) e^{-r/R_d} \right] \quad (2.3)$$

with the disc scalelength,  $R_d$  given by  $R_d = \lambda r_{200}(j_d/m_d)(1/\sqrt{2})$  assuming a non-evolving specific angular momentum parameter ( $j_d/m_d \approx 1$ ) and spin parameter ( $\lambda = 0.03$ ). The total disc mass  $M_d$  is given by  $M_d = m_d V_c^3 / 10GH(z)$ , where  $V_c$  is the circular velocity of the halo and  $H(z)$  is the Hubble constant at redshift  $z$ . The stellar mass is assumed to reside primarily in the disc, ( $m_d = M_*/M_{\text{halo}}$ ), with  $M_*$  being the average stellar mass in the halo computed from the relation of ref. [14]. The black hole is assumed to be a central point source with mass  $M_{\text{BH}}$  given by ref. [12].

## 3 Results

Figure 1 shows the above three components at  $z \sim 6$  for three representative dark matter halos with masses  $M_{\text{halo}} = 10^{10}, 10^{11}$  and  $10^{12} M_{\odot}$ , respectively. The inferred total stellar masses  $M_*$  from ref. [14] are indicated on each panel, as well as the corresponding UV magnitudes,  $M_{\text{UV}}$  obtained from the observationally derived relation of ref. [27]. Our predicted disc radii evolve as  $(1 + z)^{\beta}$  with  $\beta \approx -1$  for this stellar mass range, consistent with the findings from the CANDELS [29] and HST/Hubble Frontier Fields [30, 31] galaxy observations at  $z \sim 6$ –8. The black hole masses in these galaxies predicted from ref. [12] are  $\log_{10}(M_{\text{BH}}/M_{\odot}) = 6.3, 8.0, 9.7$ , implying  $M_{\text{BH}}/M_* \approx 0.3$ –0.4. The figure shows rotational circular velocities,  $v_{\text{rot},i} = (GM_i(r)/r)^{1/2}$  as a function of radial distance  $r$ , where

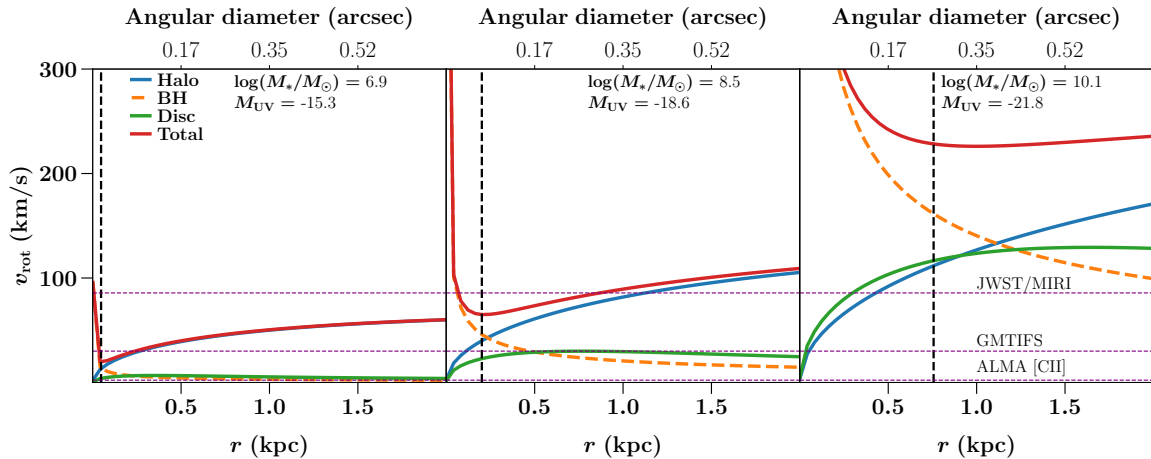


**Figure 1.** Rotation curves around three typical dark matter haloes (with masses  $M_{\text{halo}} = 10^{10}, 10^{11}$  and  $10^{12} M_{\odot}$  respectively from left to right) at  $z = 6$ . The halo is assumed to follow a Navarro-Frenk-White [25] profile with a concentration parameter [26]  $c = 3.5$ , and contains a central supermassive black hole, with mass  $M_{\text{BH}}$ , and an exponential stellar disc with spin parameter  $\lambda = 0.03$  (the inferred total stellar mass  $M_*$  is also indicated, along with the corresponding UV magnitude,  $M_{\text{UV}}$  obtained from the relation of ref. [27]). The circular velocities  $v_{\text{rot}}$  (in km/s) induced by the black hole (orange dashed lines), stellar disc (green solid lines) and dark matter halo (blue solid lines) are plotted along with the total circular velocity (red solid line). The central dominance of the black hole leads to a visible Keplerian correction in the otherwise flat rotation curve within the inner  $< 1$  kpc. Vertical dashed lines in each panel indicate  $R_{\text{inf}}$ , the radius of influence at which  $M_{\text{BH}} = M_{\text{halo}}(R_{\text{inf}}) + M_{\text{d}}(R_{\text{inf}})$ . Horizontal dashed lines indicate the maximum spectral resolutions achievable by several current and upcoming facilities, such as the ALMA observing the [CII]  $158 \mu\text{m}$  transition at  $z \sim 6$ , the GMT IFS and the JWST MIRI instrument. Top horizontal axes show the angular diameter  $\theta = [2r/D_A(z)]$  corresponding to the radial distance  $r$  on the lower horizontal axis.

$i$  denotes the disc, black hole or halo component. The total circular velocity, given by  $v_{\text{tot}}(r) = (\sum_i v_{\text{rot},i}(r)^2)^{1/2}$  is also plotted. A Keplerian correction to the rotation curve at the innermost  $< 1$  kpc is clearly distinguishable for stellar masses of  $10^9$ – $10^{10} M_{\odot}$ , a mass range for which sub-millimetre observations already exist in the literature [30]. The radius of influence  $R_{\text{inf}}$  of the black hole, defined as the scale at which  $M_{\text{BH}} = M_{\text{d}}(R_{\text{inf}}) + M_{\text{halo}}(R_{\text{inf}})$ , is indicated by the vertical dashed line on each panel. For the three galaxy masses considered,  $R_{\text{inf}}$  ranges from 0.05 to 0.76 kpc, corresponding to angular diameter sizes,  $\theta = (2R_{\text{inf}}/D_A)$  of  $0.01''$ ,  $0.06''$  and  $0.26''$  respectively, where  $D_A$  is the cosmological angular-diameter distance to redshift  $z = 6$ . The horizontal dashed lines show the lowest circular velocities (corresponding to the highest spectral resolutions) achievable by current and future generation instruments, including (i) ALMA observing the [CII] transition at  $z \sim 6$  with channel widths of  $\sim 2 \text{ MHz} \approx 2.2 \text{ km/s}$  [e.g., ref. 32], (ii) the Giant Magellan Telescope (GMT)<sup>3</sup> Integral Field Spectrometer (GMTIFS)<sup>4</sup> with a spectral resolution of  $R \sim 10000$  corresponding to  $\sim 30 \text{ km/s}$ , and (iii) the James Webb Space Telescope (JWST)<sup>5</sup> whose Mid-InfraRed Instrument [MIRI; e.g. ref. 33] has a resolving power of  $R = \delta\lambda/\lambda \sim 3500$  corresponding to  $\sim 85.7 \text{ km/s}$ .

<sup>3</sup><https://www.gmto.org/>.

<sup>4</sup><https://www.gmto.org/resources/near-ir-ifu-and-adaptive-optics-imager-gmtifs/>.

<sup>5</sup><https://www.jwst.nasa.gov/>.

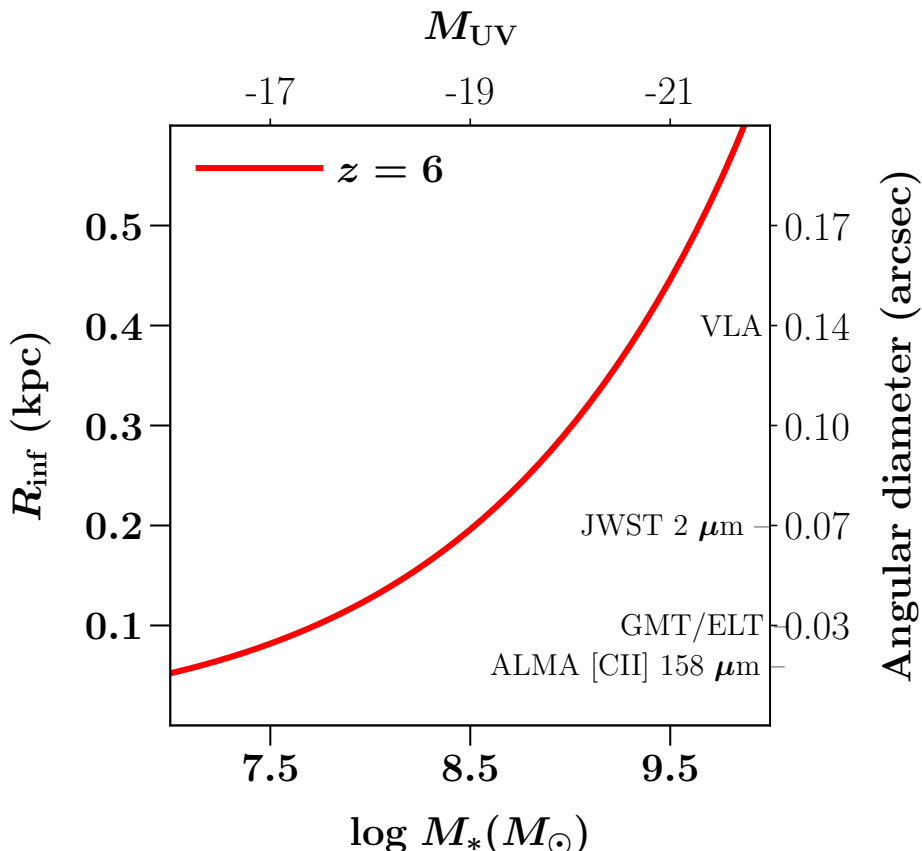


**Figure 2.** Evolution of the radius of influence,  $R_{\text{inf}}$ , of the central black hole as a function of the surrounding stellar mass,  $M_*$  (lower horizontal axis) and the corresponding absolute magnitude,  $M_{UV}$  of the host galaxy (upper horizontal axis) at  $z = 6$ , assuming the same dark matter halo, stellar disc and central black hole properties as in figure 1. The right-hand vertical axis indicates the corresponding angular diameter scale  $\theta = [2R_{\text{inf}}/D_A(z = 6)]$ , on which the angular resolutions of several upcoming facilities at these redshifts (ALMA in its most extended configuration observing [CII] 158  $\mu\text{m}$ , the GMT/ELT, JWST and VLA observing the CO 1 – 0) are indicated.

The main result of figure 1 is the red curve, which indicates the influence of the black hole on the kinematics of the stellar disc. Although the figure illustrates this for the stellar component, it is important to note that *any* tracer of the underlying dark matter halo can be used to infer the mass of the black hole from its radius of influence.

The evolution of  $R_{\text{inf}}$  with stellar mass is shown in figure 2. The figure shows that  $R_{\text{inf}}$  evolves strongly with stellar masses in the range  $10^7$ – $10^{10} M_\odot$  at  $z \sim 6$ , as can also be seen from figure 1. The upper  $x$ -axis shows the absolute magnitudes ( $M_{UV}$ ) corresponding to this mass range, computed from the relation of ref. [27] at  $z = 6$ .

Figure 3 shows  $R_{\text{inf}}$  at three different halo masses ( $\log_{10}(M_{\text{halo}}/M_\odot) = 10, 11, 11.5$ ) across the range  $z \sim 5$ –8. This halo mass range corresponds to a stellar mass range of  $\log_{10}(M_*/M_\odot) \approx 6.9$ –9.3, which is accessible to HST at these redshifts [31]. The near-constant black hole-stellar mass relation in this  $z$ -range implies that  $R_{\text{inf}}$  does not evolve much with redshift for a given halo mass.

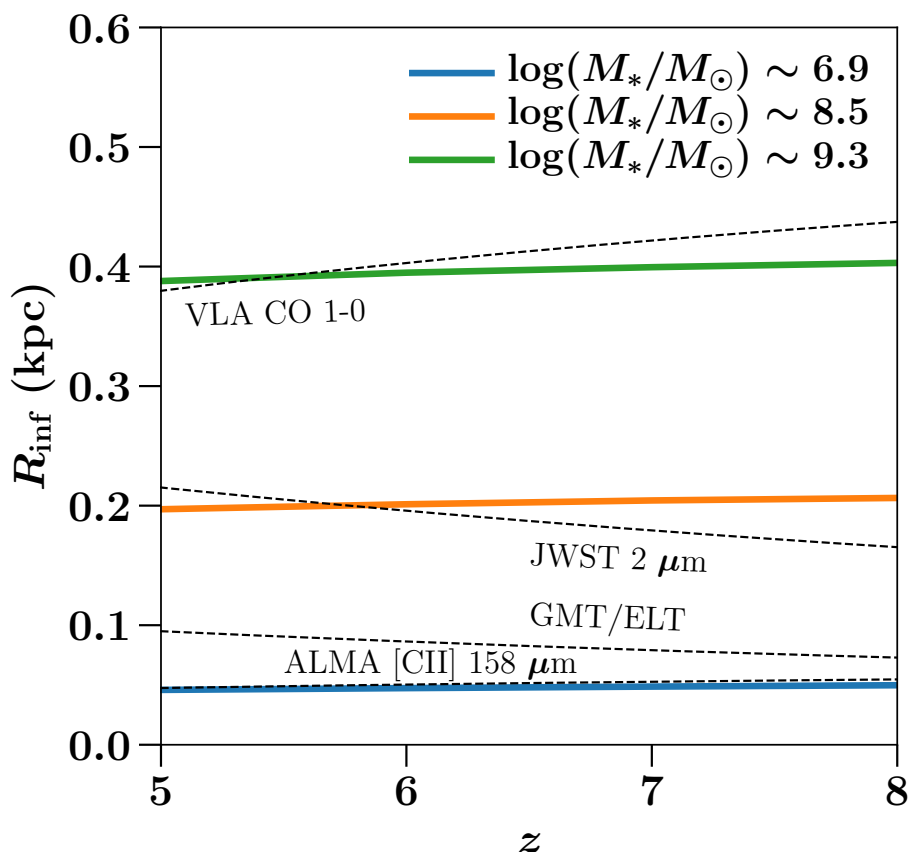


**Figure 3.** Evolution of the black hole radius of influence  $R_{\text{inf}}$  with  $z$  for three different halo masses ( $\log_{10}(M_{\text{halo}}/M_{\odot}) = 10, 11$  and  $11.5$  respectively, corresponding to the inferred stellar mass range  $\log_{10}(M_*/M_{\odot}) \approx 6.9\text{--}9.3$ ). The angular resolutions achievable by several current and future facilities (ALMA in its most extended configuration observing [CII]  $158\ \mu\text{m}$ , the GMT/ELT, JWST and VLA observing the CO  $1-0$ ) are overplotted as dashed lines.

For the highest stellar masses, the black hole can dominate the kinematics up to a distance  $> 0.5\text{ kpc}$ , which corresponds to an angular scale of  $> 0.2''$ . These values are well within the reach of current and upcoming observations, the angular resolutions of some of which are indicated on figures 2 and 3. Many observatories in the next generation of ground-based telescopes (GMT, as well as ELT,<sup>6</sup> and TMT<sup>7</sup>) will have adequate spatial resolution ( $\lesssim 30\text{ mas}$ ) to search for these black holes. ALMA in its extended 12-m configuration should be able to detect [CII]-emitting galaxies with  $0.02\text{--}0.043''$  resolution at frequencies corresponding to  $z \sim 6\text{--}10$ , and the JWST should be able [34] to resolve at least  $\sim 200$  such galaxies at  $z \sim 8$ , with a resolution of  $\sim 68\text{ mas}$  at  $2\ \mu\text{m}$ .<sup>8</sup> Further, the VLA<sup>9</sup> and the Phase II of the planned Square Kilometre Array [SKA; 35] will be able to access the CO J  $1 \rightarrow 0$  transition at redshifts  $z \sim 6\text{--}10$  with angular resolutions of  $0.2\text{--}0.3''$ , which could potentially resolve  $R_{\text{inf}}$  of the central black hole in the brightest galaxies at these epochs.

<sup>6</sup><https://www.eso.org/sci/facilities/eelt/>.

<sup>7</sup><https://www.tmt.org/>.

<sup>8</sup><https://sci.esa.int/web/jwst/-/47519-gardner-j-et-al-2009>.

<sup>9</sup><https://science.nrao.edu/facilities/vla/>.

## 4 Conclusions

These predictions have far-reaching implications. First, a direct *kinematic* measurement of the central black hole masses will enable key physics insights into the growth and merger histories of supermassive black holes in the earliest galaxies. It would also shed light on the active phases (‘duty cycles’) of the earliest black holes, and permit exciting constraints on the currently debated contribution of quasars to cosmic reionization of hydrogen and helium [36]. It has been recently suggested that a significant population of strongly lensed quasars [37, 38] in the early universe may have been missed by current surveys due to selection effects that rule out bright lenses [39]. Direct black hole mass measurements form a complementary dataset to aid detections of lensed quasars from future surveys. Finally, a characterization of the black hole mass function will enable forecasting of future measurements of gravitational radiation emitted by pairs of these produced by galaxy mergers [40], in anticipation of the upcoming Laser Interferometer Space Antenna (*LISA*<sup>10</sup>).

## Acknowledgments

The work of AL was supported in part by Harvard’s Black Hole Initiative, which is funded by grants from JTF and GBMF. We thank the anonymous referee for a detailed and helpful report that improved the content and the quality of presentation.

## References

- [1] A.M. Ghez et al., *Stellar orbits around the galactic center black hole*, *Astrophys. J.* **620** (2005) 744 [[astro-ph/0306130](#)] [[INSPIRE](#)].
- [2] A.M. Ghez et al., *Measuring Distance and Properties of the Milky Way’s Central Supermassive Black Hole with Stellar Orbits*, *Astrophys. J.* **689** (2008) 1044 [[arXiv:0808.2870](#)] [[INSPIRE](#)].
- [3] R. Genzel, C. Pichon, A. Eckart, O.E. Gerhard and T. Ott, *Stellar dynamics in the Galactic centre: Proper motions and anisotropy*, *Mon. Not. Roy. Astron. Soc.* **317** (2000) 348 [[astro-ph/0001428](#)] [[INSPIRE](#)].
- [4] R. Schodel, T. Ott, R. Genzel, A. Eckart, N. Mouawad and T. Alexander, *Stellar dynamics in the central arcsecond of our Galaxy*, *Astrophys. J.* **596** (2003) 1015 [[astro-ph/0306214](#)] [[INSPIRE](#)].
- [5] M. Miyoshi et al., *Evidence for a black hole from high rotation velocities in a subparsec region of NGC4258*, *Nature* **373** (1995) 127 [[INSPIRE](#)].
- [6] J. Kormendy and L.C. Ho, *Coevolution (Or Not) of Supermassive Black Holes and Host Galaxies*, *Ann. Rev. Astron. Astrophys.* **51** (2013) 511 [[arXiv:1304.7762](#)] [[INSPIRE](#)].
- [7] A.E. Reines and M. Volonteri, *Relations between Central Black Hole Mass and Total Galaxy Stellar Mass in the Local Universe*, *Astrophys. J.* **813** (2015) 82 [[arXiv:1508.06274](#)].
- [8] E. Bañados et al., *An 800-million-solar-mass black hole in a significantly neutral Universe at redshift 7.5*, *Nature* **553** (2018) 473 [[arXiv:1712.01860](#)] [[INSPIRE](#)].
- [9] K. Inayoshi, E. Visbal and Z. Haiman, *The Assembly of the First Massive Black Holes*, [arXiv:1911.05791](#) [[INSPIRE](#)].
- [10] R. Decarli et al., *An ALMA [CII] survey of 27 quasars at  $z > 5.94$* , *Astrophys. J.* **854** (2018) 97 [[arXiv:1801.02641](#)] [[INSPIRE](#)].

---

<sup>10</sup><https://www.lisamission.org>.



- [11] B.P. Venemans et al., *Bright [CII] and dust emission in three  $z > 6.6$  quasar host galaxies observed by ALMA*, *Astrophys. J.* **816** (2016) 37 [[arXiv:1511.07432](#)] [[INSPIRE](#)].
- [12] J.S.B. Wyithe and A. Loeb, *A Physical model for the luminosity function of high-redshift quasars*, *Astrophys. J.* **581** (2002) 886 [[astro-ph/0206154](#)] [[INSPIRE](#)].
- [13] D.J. Croton, *A simple model to link the properties of quasars to the properties of dark matter halos out to high redshift*, *Mon. Not. Roy. Astron. Soc.* **394** (2009) 1109 [[arXiv:0901.4104](#)] [[INSPIRE](#)].
- [14] P. Behroozi, R.H. Wechsler, A.P. Hearin and C. Conroy, *UniverseMachine: The correlation between galaxy growth and dark matter halo assembly from  $z = 0-10$* , *Mon. Not. Roy. Astron. Soc.* **488** (2019) 3143 [[arXiv:1806.07893](#)] [[INSPIRE](#)].
- [15] H. Suh et al., *No significant evolution of relations between Black hole mass and Galaxy total stellar mass up to  $z \sim 2.5$* , [arXiv:1912.02824](#).
- [16] T.A. Davis, *A figure of merit for black hole mass measurements with molecular gas*, *Mon. Not. Roy. Astron. Soc.* **443** (2014) 911 [[arXiv:1406.2555](#)] [[INSPIRE](#)].
- [17] P. Natarajan et al., *Unveiling the First Black Holes With JWST: Multi-wavelength Spectral Predictions*, *Astrophys. J.* **838** (2017) 117 [[arXiv:1610.05312](#)] [[INSPIRE](#)].
- [18] T.R. Lauer, S. Tremaine, D. Richstone and S.M. Faber, *Selection Bias in Observing the Cosmological Evolution of the  $M_\bullet$ - $\sigma$  and  $M_\bullet$ - $L$  Relationships*, *Astrophys. J.* **670** (2007) 249 [[arXiv:0705.4103](#)] [[INSPIRE](#)].
- [19] A. Schulze and L. Wisotzki, *Selection effects in the black hole-bulge relation and its evolution*, *Astron. Astrophys.* **535** (2011) A87 [[arXiv:1109.2787](#)] [[INSPIRE](#)].
- [20] A. Schulze and L. Wisotzki, *Accounting for selection effects in the BH-bulge relations: no evidence for cosmological evolution*, *Mon. Not. Roy. Astron. Soc.* **438** (2014) 3422 [[arXiv:1312.5610](#)] [[INSPIRE](#)].
- [21] C.J. Willott, J. Bergeron and A. Omont, *A Wide Dispersion in Star Formation Rate and Dynamical Mass of  $10^8$  Solar Mass Black Hole Host Galaxies at Redshift 6*, *Astrophys. J.* **850** (2017) 108 [[arXiv:1710.02212](#)].
- [22] C. DeGraf, T. Di Matteo, T. Treu, Y. Feng, J.H. Woo and D. Park, *Scaling relations between black holes and their host galaxies: comparing theoretical and observational measurements and the impact of selection effects*, *Mon. Not. Roy. Astron. Soc.* **454** (2015) 913 [[arXiv:1412.4133](#)] [[INSPIRE](#)].
- [23] K.-W. Huang, T. Di Matteo, A.K. Bhowmick, Y. Feng and C.-P. Ma, *BLUETIDES simulation: establishing black hole-galaxy relations at high redshift*, *Mon. Not. Roy. Astron. Soc.* **478** (2018) 5063 [[arXiv:1801.04951](#)].
- [24] M.A. Marshall, S.J. Mutch, Y. Qin, G.B. Poole and J.S.B. Wyithe, *Dark-ages reionization and galaxy formation simulation — XVIII. The high-redshift evolution of black holes and their host galaxies*, [arXiv:1910.08124](#).
- [25] J.F. Navarro, C.S. Frenk and S.D.M. White, *The Structure of cold dark matter halos*, *Astrophys. J.* **462** (1996) 563 [[astro-ph/9508025](#)] [[INSPIRE](#)].
- [26] B. Diemer and M. Joyce, *An accurate physical model for halo concentrations*, *Astrophys. J.* **871** (2019) 168 [[arXiv:1809.07326](#)] [[INSPIRE](#)].
- [27] S. Tacchella, S. Bose, C. Conroy, D.J. Eisenstein and B.D. Johnson, *A Redshift-independent Efficiency Model: Star Formation and Stellar Masses in Dark Matter Halos at  $z \gtrsim 4$* , *Astrophys. J.* **868** (2018) 92 [[arXiv:1806.03299](#)] [[INSPIRE](#)].
- [28] H.J. Mo, S. Mao and S.D.M. White, *The Formation of galactic disks*, *Mon. Not. Roy. Astron. Soc.* **295** (1998) 319 [[astro-ph/9707093](#)] [[INSPIRE](#)].



- [29] R. Kawamata, M. Ishigaki, K. Shimasaku, M. Oguri, M. Ouchi and S. Tanigawa, *Size-Luminosity Relations and UV Luminosity Functions at  $z = 6-9$  Simultaneously Derived from the Complete Hubble Frontier Fields Data*, *Astrophys. J.* **855** (2018) 4 [[arXiv:1710.07301](#)].
- [30] T. Shibuya, M. Ouchi, Y. Harikane and K. Nakajima, *Morphologies of  $\sim 190,000$  Galaxies at  $z = 0-10$  Revealed with HST Legacy Data. III. Continuum Profile and Size Evolution of Ly $\alpha$  Emitters*, *Astrophys. J.* **871** (2019) 164.
- [31] B.W. Holwerda, R. Bouwens, P. Oesch, R. Smit, G. Illingworth and I. Labbe, *The Sizes of Candidate  $z = 9-10$  Galaxies: Confirmation of the Bright CANDELS Sample and Relation with Luminosity and Mass.*, *Astrophys. J.* **808** (2015) 6 [[arXiv:1406.1180](#)].
- [32] S. Carniani et al., *Extended ionised and clumpy gas in a normal galaxy at  $z = 7.1$  revealed by ALMA*, *Astron. Astrophys.* **605** (2017) A42 [[arXiv:1701.03468](#)].
- [33] G.S. Wright et al., *The Mid-Infrared Instrument for the James Webb Space Telescope, II: Design and Build*, *Publ. Astron. Soc. Pac.* **127** (2015) 595 [[arXiv:1508.02333](#)].
- [34] M. Vogelsberger et al., *High redshift JWST predictions from IllustrisTNG: Dust modelling and galaxy luminosity functions*, [arXiv:1904.07238](#).
- [35] A.R. Taylor, *The Square Kilometre Array*, in *Neutron Stars and Pulsars: Challenges and Opportunities after 80 years*, J. van Leeuwen ed., *IAU Symp.* **291** (2013) 337.
- [36] P. Madau and F. Haardt, *Cosmic Reionization after Planck: Could Quasars Do It All?*, *Astrophys. J.* **813** (2015) L8 [[arXiv:1507.07678](#)] [[INSPIRE](#)].
- [37] X. Fan et al., *The Discovery of a Gravitationally Lensed Quasar at  $z = 6.51$* , *Astrophys. J. Lett.* **870** (2019) L11 [[arXiv:1810.11924](#)].
- [38] J.S.B. Wyithe and A. Loeb, *Gravitational lenses magnify up to one third of the most distant quasars*, *Nature* **417** (2002) 923 [[astro-ph/0203116](#)] [[INSPIRE](#)].
- [39] F. Pacucci and A. Loeb, *Most Lensed Quasars at  $z > 6$  are Missed by Current Surveys*, *Astrophys. J.* **870** (2019) L12 [[arXiv:1810.12302](#)] [[INSPIRE](#)].
- [40] A.D. Goulding, K. Pardo, J.E. Greene, C.M.F. Mingarelli, K. Nyland and M.A. Strauss, *Discovery of a Close-separation Binary Quasar at the Heart of a  $z \sim 0.2$  Merging Galaxy and Its Implications for Low-frequency Gravitational Waves*, *Astrophys. J.* **879** (2019) L21 [[arXiv:1907.03757](#)] [[INSPIRE](#)].